EXPERIMENTATION AND NUMERICAL MODELLING OF NANOINDENTATION OF FIBROUS COMPOSITES

M. Hardiman[1], C.T. McCarthy[1*]

[1] *Materials and Surface Science Institute, University of Limerick, Address*
**conor.mccarthy@ul.ie*

Keywords: Nanoindentation, Carbon-Fibre-Reinforced-Polymer, Finite-Element-Analysis

Abstract

The nanoindentation process applied to fibrous composite microstructures has been analysed both experimentally and numerically using finite element models. Nanoindentation experiments have been carried out on the microstructure of the high strength, high fibre volume-fraction HTA/6376 composite in an attempt to determine the mechanical properties of the constituent materials in-situ. The deviation of the experimental results from the expected values was investigated by finite element modelling of the nanoindentation process applied to fibrous composites. The results from the models showed that when indenting the individual composite constituents, the indentation response was affected by the neighbouring constituent. This highlights the inherent difficulty of determining the properties of the "interphase" region in high volume-fraction composites.

1 Introduction

In recent years, a large amount of research in the area of composite materials has been focused on analysing the response of the material's constituent phases and their interfaces under various loading conditions. Analysis of this type involves examining the microstructure of the composite material and relating the observed behaviour to macroscopic failure mechanisms. Most micromechanical models which are used to predict this behaviour assume that the properties of the constituent materials in-situ are the same as the properties of the bulk materials [1, 2]. Recent studies have shown that these properties can vary significantly from their bulk properties after the composite manufacturing process. Also, of particular interest when generating models of this nature is the interface between the fibres and the matrix material. Studies at the nanoscale can provide useful information about the size and strength of the interphase region which is of particular importance when attempting to accurately model the failure initiation and propagation of fibrous composites under various loading conditions.

Nanoindentation is a technique which is commonly used to determine material properties such as hardness and elastic modulus at the micro and nanoscales [3]. Previous authors have shown that the elastic modulus of the matrix material can potentially change after the composite

curing process by up to 30% [4]. Efforts have also been made to characterise the fibre-matrix interface between the fibres and the matrix by carrying out nanoindentation tests close to the interface. These experiments show a distinct 'interphase' region where the indentation modulus gradually changes from the resin properties to the fibre properties [5,6]. These studies have noted the potential influence of the surrounding fibres on the indentation load-displacement data and in an effort to avoid this constraining effect, the experimental indentation depths were kept as low as possible; however, no quantitative analysis of this effect were carried out.

In this study, preliminary nanoindentation experiments were carried out on the microstructure of the HTA/6376 high-strength composite in an attempt to determine the in-situ mechanical properties of the constituent materials, namely the HTA fibres and 6376 epoxy matrix. The nanoindentation of the fibrous composite microstructure has then been modelled in order gain a greater insight into the technique when applied to this material and to better understand the significance of the experimental results. Due to the inherent difficulties that are encountered when attempting to carry out nanoindentation tests on a high-volume fraction composite, the procedure for co-curing specialised samples of the HTA/6376 together with bulk 6376 matrix is described as well as its benefits for the future experimental work of the current project.

2 Nanoindentation Theory

Nanoindentation tests involve pushing a diamond tipped indenter head into a bulk material under either load or displacement control. The displacement is monitored as a function of the load throughout the load-unload cycle. A typical load-displacement curve is shown in Figure 1, where h_p is the depth of the residual plastic impression and h_e is the depth of elastic recovery.

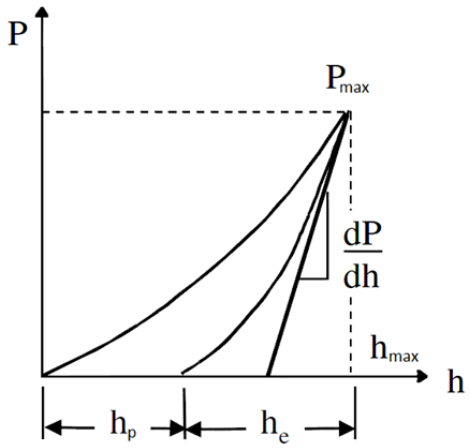

Figure 1. Typical Nanoindentation load-displacement curve

When determining material properties such as hardness and elastic modulus a three-sided pyramid indenter known as Berkovich indenter is commonly used. The method of interpreting nanoindentation data has been developed over a number of years with the Oliver and Pharr [7] method being the most extensively used method of determining modulus and hardness. Hardness (H) is defined as the contact pressure under the indenter:

$$H = \frac{P}{A_c} \tag{1}$$

where P is the indenter load and A_c is the projected contact area calculated at a depth of indentation, *h*. The initial slope of the unloading curve can be related to the reduced elastic modulus of the contact using Equation 2:

$$S = \frac{dP}{dH} = \frac{2E_r\sqrt{A_c}}{\sqrt{\pi}} \tag{2}$$

where S is the initial slope of the unloading curve or contact stiffness, P is the applied load and E_r is the reduced modulus. As the measured displacement in a nanoindentation experiment is a combination of the displacement of the indenter tip as well as the specimen, the specimen modulus (E_s) can be related to the reduced modulus (E_r) using Equation 3, provided the indenter modulus (E_i) is known and the Poisson's ratios of the specimen and indenter (ν_s and ν_i respectively) are known or can be estimated:

$$\frac{1}{E_r} = \frac{1-\nu_s^{\,2}}{E_s} + \frac{1-\nu_i^{\,2}}{E_i} \tag{3}$$

3 Experimental Results

Nanoindentation experiments were carried out on the constituent materials of the HTA/6376 composite in an attempt to determine their in-situ mechanical properties. These results could then be compared with the values of the elastic properties of the constituents in their bulk form, which are shown in Table 1.

	Fibre (HTA)	**Matrix (6376)**
E_{11} (GPa)	238	3.63
E_{22}/E_{33} (GPa)	28	
ν_{12}	0.28	0.34
ν_{23}	0.33	
ν_{31}	0.02	
G_{12} (GPa)	24	
G_{23} (GPa)	7.2	
G_{31} (GPa)	24	

Table 1. Elastic properties of the HTA/6376 composite constituent materials in their bulk form [8, 9].

A series of indentations were carried out in large resin pockets in the composite in an attempt to determine the in-situ mechanical properties of the matrix constituent. These resin pockets

were located in the interply regions of the composite as shown in Figure 2. The indentations were carried out under load-control up to a maximum load of 5mN. The load was then held constant at this maximum load for 5 seconds in an attempt to reduce the effect of viscoelasticity on the indentation modulus results, before being unloaded. A total of five indentations were carried out into these resin pockets leading to an average indentation modulus value of 9.346 GPa with a standard deviation of 0.322. Two of the five indentations are highlighted and shown on a micrograph Figure 2a.

A series of indentations were also carried out into the centre of the HTA fibres under load control up to a maximum load of 15mN. In total, five indentations were carried out. The mean indentation modulus value from these five indentations was calculated using the Oliver and Pharr method was 56.557 GPa with a standard deviation of 0.752 GPa. The selected fibres are shown targeted using an optical microscope in Figure 2b.

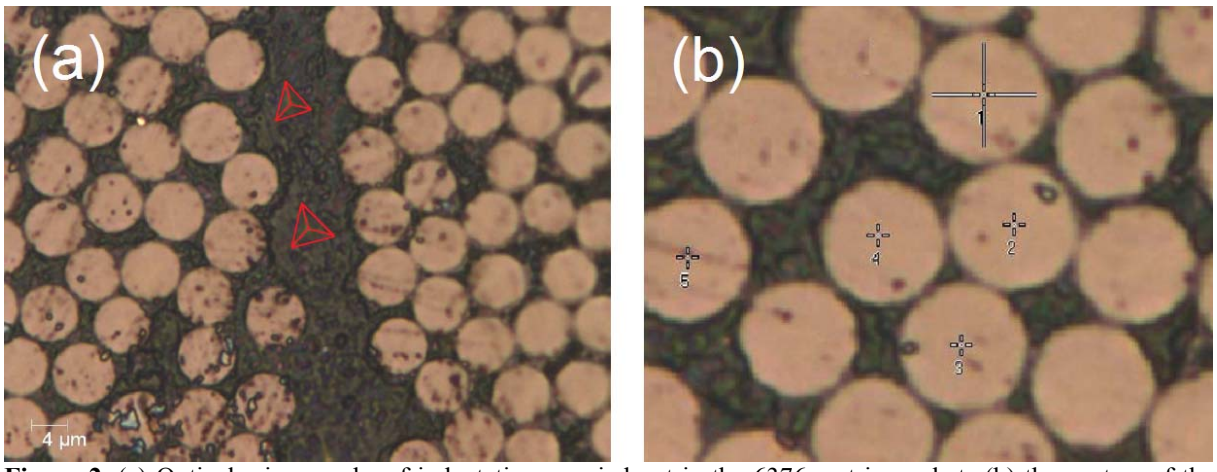

Figure 2. (a) Optical micrographs of indentations carried out in the 6376 matrix pockets (b) the centres of the HTA fibres

4 Finite Element Analysis

4.1 Material Definition

In order to investigate the relevance of the experimental results, the elastic-plastic nanoindentation process was modelled using a number of 2D and 3D models. The commercial finite-element software ABAQUS v6.10 [8] was used to create the models and carry out the analyses. A large strain solution was used and both materials were defined using the mechanical properties shown in Table 1. The HTA fibre was assumed to exhibit transversely isotropic linear elastic behaviour, while the 6376 resin was assumed to exhibit elastic-perfectly plastic material behaviour. The yield behaviour of the epoxy matrix was modelled using the pressure-sensitive Mohr-Coulomb yield criterion. The Mohr-Coulomb criterion induces yield when the combined normal (σ_n) and shear stresses (τ) reach a critical level according to Equation 4:

$$\tau_c = \tau + \sigma_n \tan\phi \qquad (4)$$

where τ_c is the cohesion stress (yield stress in pure shear) and ϕ is the angle of internal friction.

4.2 Investigation of Matrix Results

In order to investigate the surprisingly large mean experimental indentation modulus value for the in-situ 6376 matrix constituent, finite element models of the indentation process were used. The mean experimental indentation modulus value was determined to be 9.346 GPa which is roughly two and a half times larger than the value for the bulk 6376 matrix material. In order to determine if the fibres surrounding the indentation area had an effect on the load-displacement data, 3D finite element models were used. An example of the model used is shown in Figure 3. The Berkovich three-sided pyramid indenter geometry used in the experiments has six-fold symmetry and this has been used in the modelling procedure to simplify the analysis. The indenter has been modelled as a rigid plane with an angular offset from the surface of the specimen which perfectly represents the Berkovich geometry.

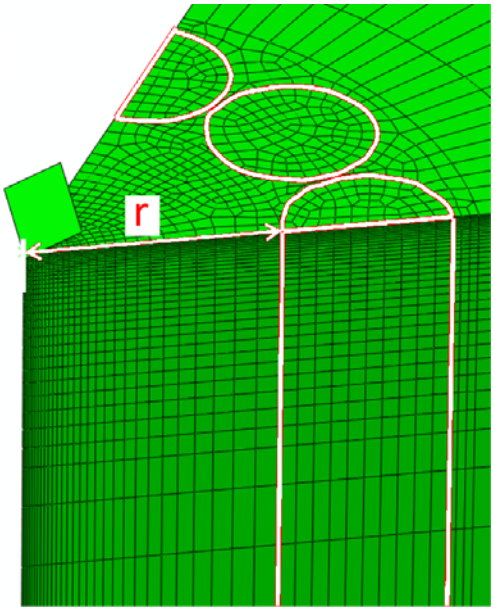

Figure 3. 3D finite element model with fibres represented by a circular pattern of closely-packed fibres

The material being indented has been defined using the 6376 matrix mechanical properties, the cylindrical sections (highlighted in Figure 3) have been defined using the HTA fibre properties, while the material further afield from this region has been defined using the bulk properties of the HTA/6376 composite through an embedded cell approach. The diameter of the HTA fibres measured 6.6μm while the inter-fibre spacing measured 0.5μm. These values were chosen based on average results determined in a previous study, which characterised the fibre distribution of the HTA/6376 composite microstructure [9]. The value of *r* shown in Figure 3 represents the distance from the initial contact point of indentation to the outside fibre region. This value of *r* was varied and the indentation depth held constant at 1μm, in order to determine the change in indentation response closer to the rigid boundary.

4.3 Investigation of Fibre Results

The mean experimental indentation modulus for the fibre constituent was 56.557 GPa, which is much lower than the value of modulus in the longitudinal direction determined from

experiments (238 GPa). A 2D axisymmetric representation of the indentation process was used to investigate this apparent discrepancy in the experimental results. The indenter has been represented as a rigid cone with a half-angle of 70.3° which gives the same projected area to depth ratio as the three-sided Berkovich indenter used in the nanoindentation experiments. The first model, shown in Figure 4a, applied the anisotropic fibre properties to the bulk indented material in order to determine if the experimental indentation modulus values could be explained by the fibre's anisotropic properties. The 2nd model shown in Figure 4b has both fibre and matrix sections which are defined using the properties in Table 1. This model will determine whether the surrounding matrix material had an effect on the experimental indentation modulus result for the fibre constituent. Here the average fibre diameter and indentation depths from the experiments were used for the simulation.

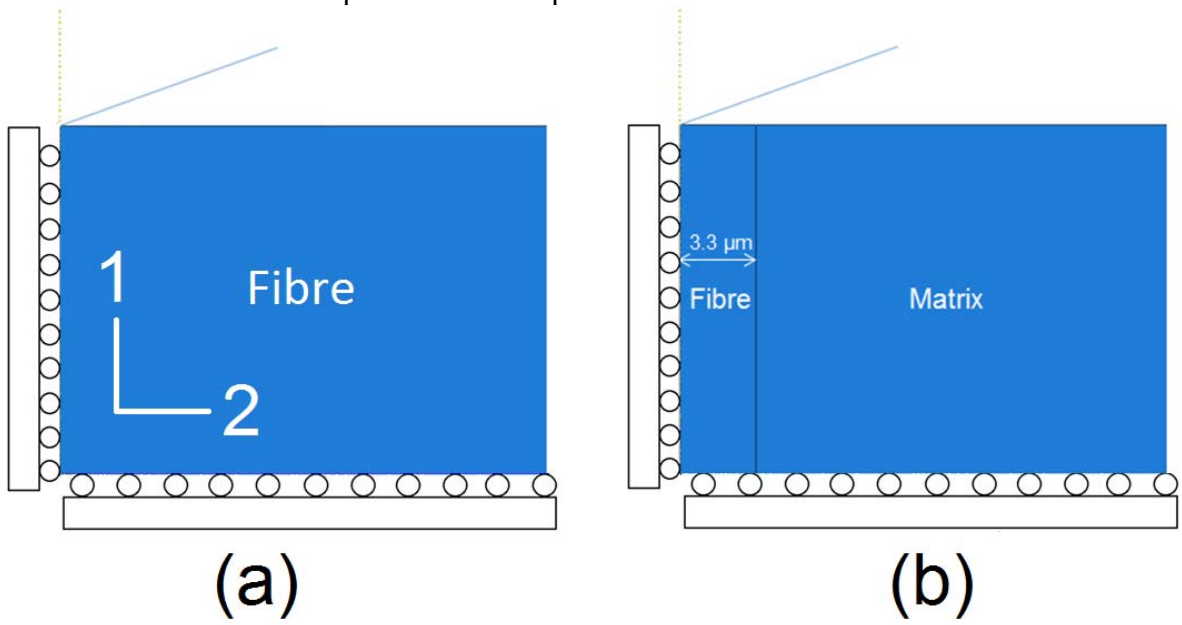

Figure 4. 3D finite element model with fibres represented by a circular pattern of closely-packed fibres

5 Results and Discussion

In order to investigate the effect that the surrounding fibres had on the indentation modulus of the matrix constituent, the values of Young's modulus obtained for each value of *r* were compared with the unconstrained value of Young's modulus obtained from the same model. The uncontrained models were models without the fibre sections and embedded cell. This gave an indication as to how much the constraints were affecting the value of indentation modulus calculated using the nanoindentation simulation's load-displacement data. The ratio of Young's Modulus to unconstrained Young's modulus is plotted against values of *r* in Figure 5.

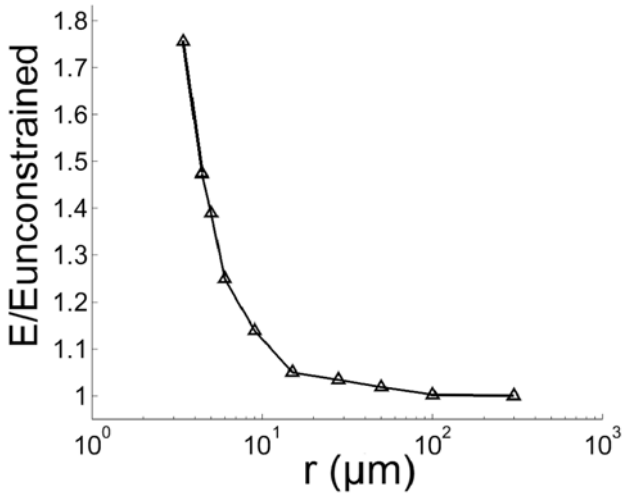

Figure 5. Ratio of Young's Modulus to unconstrained Young's modulus plotted against r

Figure 5 shows that as the indentations come closer to the fibre region (i.e. the value of *r* becomes smaller), the value of indentation modulus becomes larger in comparison the unconstrained indentation modulus. This shows that the fibre constraint did have an effect on the experimental results for the matrix. However, it does not fully explain the 2.5x rise in indentation modulus. This would appear to indicate that the modulus of the 6376 matrix does increase somewhat due to the composite curing process and warrants further experimental investigation. This gradient in elastic modulus as indentations are carried out closer to the fibre also highlights the inherent difficulty in determining properties of the "interphase" region in high volume-fraction composites.

The experimental fibre indentation results were investigated initially by modelling the indentation of bulk material defined using the fibre's anisotropic properties. The load-displacement data for this model resulted in an indentation modulus of 135 GPa. This was much lower than the longitudinal modulus value of the material in the literature (238 GPa) which was used to define the material in the models. The indentation modulus value most likely contains influences from both the longitudinal (E_{11}) and transverse (E_{22}) moduli making it difficult to quantify. The second model where the indented fibre is modelled surrounded by matrix material produced an indentation modulus value of 52.9 GPa. This value is reasonably close to the mean of the experimentally determined values (56.5 GPa) which suggests that the low value of experimental indentation modulus is due to a combination of the fibre anisotropic properties and an added compliance due to the surrounding softer matrix material.

7 Conclusions

The combined experimental and numerical analysis shows that the load-displacement data from indentations carried out on the constituent materials of a fibrous composite are affected by the neighbouring constituents. The matrix (6376) indentations were affected by the constraining effect of the surrounding fibres and the fibre indentations (HTA) were affected by the compliance of the surrounding matrix material as well as their anisotropic material properties. The models provide an insight into the mechanics of the indentation experiment applied to fibrous composites.

Acknowledgments

The authors wish to acknowledge the funding provided by the Irish Research Council for Science, Engineering and Technology (IRCSET). The authors would also like to acknowledge the nanoindenter supplier CSM Instruments for carrying out the experiments and providing the results. Computations were carried out using the SFI/HEA Irish Centre for High-End Computing (ICHEC) whom the authors wish to acknowledge for the provision of computational facilities and support.

References

[1] T.J. Vaughan, C.T. McCarthy, Composites Science and Technology, **71** 388-396 (2011).
[2] C. González, J. Llorca, Composites Science and Technology, **67** 2795-2806 (2007).
[3] A.C. Fischer-Cripps, Surface and Coatings Technology, **200** 4153-4165 (2006).
[4] J.R. Gregory, S.M. Spearing, Composites Science and Technology, **65** 595-607 (2005).
[5] A. Hodzic, S. Kalyanasundaram, J.K. Kim, A.E. Lowe, Z.H. Stachurski, Micron, **32** 765-775 (2001).
[6] S.-H. Lee, S. Wang, G.M. Pharr, H. Xu, Composites Part A: Applied Science and Manufacturing, **38** 1517-1524 (2007).
[7] Oliver WC, Pharr GM. An improved technique for determining hardness and elastic modulus using load and displacement sensing indentation experiments. J Mater Res **7**(6):1564–83 (1992).
[8] ABAQUS, Version 6.10EF. HKS., 2010
[9] T.J. Vaughan, C.T. McCarthy, Composites Science and Technology, **70** 291-297 (2010).